



University of Plymouth
School of Computing

Controlling the Irregularity of Spike trains

G. Bugmann

Research Report *NRG-95-04*

June 1995



Neurodynamics Research Group

Effect of Partial Reset on the Irregular Firing and the Gain of a Spiking Neuron Model.

Guido Bugmann

School of Computing, University of Plymouth, Plymouth PL4 8AA, United Kingdom

31 August 1995

Contents

| | |
|---|-----------|
| 1. Introduction | 2 |
| 2. Simulation of the extended LIF model | 4 |
| 2.1 Summary of the model | |
| 2.2 Saturating probabilistic synapses and dendritic propagation | |
| 2.3 Leaky integrator | |
| 2.4 Firing, partial reset and refractory time | |
| 2.5 Simulation of the inputs | |
| 3. Results | 7 |
| 3.1 Simulation procedure | |
| 3.2 Effect of partial reset on the irregularity of spike trains | |
| 3.3 Effects of partial reset on the interspike interval distribution | |
| 3.4 Effects of partial reset on the gain of the neuron | |
| 3.5 Role of the dendritic location of the inputs | |
| 4. Modelling the effects of partial reset | 13 |
| 4.1 Time-dependent threshold an the clustering hypothesis | |
| 4.2 Effects of temporal clustering on the statistics of spike trains | |
| 4.3 Effects of temporal clustering on the interspike interval distribution | |
| 4.4 Effects of temporal clustering on the gain of the neuron | |
| 5. Discussion | 18 |
| 5.1 Role of the features of the model in controlling the irregularity of spike trains | |
| 5.2 Biological justification of partial reset | |
| 5.3 Comparison to other models | |
| 5.4 Neuronal function | |
| 6. Conclusion | 21 |
| 7. References | 22 |
| Appendix A Coefficient of variation of the interspike intervals | I |
| A.1. Case with refractory time | |
| A.2. Case with refractory time and bursting | |
| Appendix B Counting statistics | V |
| B.1. Case without refractory time or bursting | |
| B.2. Case with refractory time in the low frequency limit | |
| B.3. Case with refractory time and bursting in the low frequency limit | |

Keywords: Neuron model, synapse model, dendrite model, irregularity of spike trains, temporal integration, transfer function, partial reset, coefficient of variation, counting statistics.

Effect of Partial Reset on the Irregular Firing and the Gain of a Spiking Neuron Model.

Guido Bugmann

School of Computing, University of Plymouth, Plymouth PL4 8AA, United Kingdom
Tel: (+44) 1752 23 25 66, Fax: (+44) 1752 23 25 40, email: gbugmann@soc.plym.ac.uk

31 August 1995

Keywords: Neuron model, synapse model, dendrite model, irregularity of spike trains, temporal integration, transfer function, partial reset, coefficient of variation, counting statistics.

Abstract

The effects of partially resetting the membrane potential of an extended Leaky Integrate-and-Fire (LIF) neuron model are investigated by simulation and theoretical analysis.

The extended LIF neuron model differs from the standard LIF model by i) the use of postsynaptic currents (PSC) extended in time and modelled by an alpha function, ii) the use of a synaptic saturation mechanism [Bugmann, 1992] to limit the temporal integration of PSCs from the same synapse and iii) the use of partial reset of the membrane potential after a spike.

The reset is partial because the potential of the capacitor is not reset to zero after each spike.

Our simulations concentrated mainly on the effects of partial reset in the case of proximal inputs, using PSCs with a short duration. The results show that partial reset increases the irregularity of the spikes trains and the gain of the neuron. With a partial reset to 91% of the pre-spike potential we obtain coefficient of variations $CV(T)$ in the same range as those of cortical neurons.

Partial reset results in an effective firing threshold which is small just after spiking, and then recovers progressively towards the normal value. This increases the probability of firing a second spike just after a spike. As a consequence, when the soma is not reset, one observes that the neuron produces bursts of spikes. When the strength of reset is increased, the neuron moves into a "temporal clustering" regime with no apparent bursts but with high values of CV . With full reset, the neuron fires rather regularly as shown by [Softky and Koch, 1993].

These observations lead us to analyse the effects of partial reset in terms of a temporal clustering model in which multiple firing occurs in response to events that would cause a single spike when total reset is used. We show analytically that temporal clustering results in an increased gain of the neuron and increased values of CV and variance $VAR(N)$ of the number N of spikes counted during a given time window. The effects of partial reset on interspike interval histograms are compatible with a temporal clustering model.

1. Introduction

Spike trains are one of the very important message carriers between neurons. Their irregularity and irreproducibility has raised basic questions regarding the neural code (the message hidden in spike trains), and the neural function (producing a response to arriving messages) [Sejnowski, 1986]. In this paper we look for conditions under which models of neurons can transform irregular input spike trains into irregular output spike trains. If it turns out that only a small parameter domain allows to produce irregularities similar to those observed in biological neurons, then we may have learned something about the function of these neurons [Stein, 1967]. Previous attempts along this line have been unsuccessful. It has been reported by [Softky and Koch, 1993] and [Bugmann, 1990] that the highly irregular firing of cortical neurons cannot be reproduced by a *single* simulated neuron performing the temporal integration of EPSPs (Excitatory Post-Synaptic Potentials) generated by independent stochastic input spike trains. This result has triggered investigations into alternative ways of producing irregular spike trains, e.g. the work by [Usher et al., 1994] focusing on medium scale activity fluctuations in *networks* of spiking neurons or the model of [Zipser et al., 1993] exploiting stochastic transitions between two firing rates in a self-excitatory *cluster* of neurons (reminiscent of an older model by [Smith and Smith, 1965]). We may note that the work by [Usher et al., 1994] has not covered the high frequency range where [Softky and Koch, 1993] make their strongest claims.

Single neurons models have also been proposed. For instance [Shadlen and Newsome, 1994] exploited a random walk dynamic of the membrane potential induced by *balanced* excitatory and inhibitory inputs, to induce random firing. The concept of balancing was also introduced in [Bell et al, 1995] for a different purpose, that of keeping the membrane potential near to threshold and enabling current fluctuations to trigger spikes. Recently [Bugmann and Taylor, 1994; Bell et al, 1995] have reminded that incomplete repolarisation (or *partial reset*) of the membrane causes highly irregular firing (for older references to that approach, see [Lansky and Musila, 1991]). The *combination* of balancing and partial reset was advocated in [Tsodyks and Sejnowski, 1995]. So far however, it has not been shown that any of these mechanisms allows to reproduce the dependence between irregularity and firing rate found in cortical cells. We demonstrate here that an extended leaky integrator neuron model, using partial reset, can reproduce the irregular firing of cortical cells, as described by [Softky and Koch, 1993].

Regarding the mechanisms by which partial reset affects the irregular firing of neurons, it has been observed that when the membrane potential of a Leaky Integrate-and-Fire (LIF) model of a neuron is *not reset* after each output spike, the neuron tends to fire in bursts [Christodoulou et al., 1994; Rospar and Lansky, 1993]. The consequence of such a bursting behaviour is that the coefficient of variation (*CV*) of the spike train generally widely exceeds 1. However, when, as in Softky's and Koch's simulations, the membrane potential is *fully reset* after each spike, this leads to rather regular spike trains characterised by values of *CV* well below 1 (Perfect regularity would lead to $CV=0$ and a perfect randomness, a pure Poisson process, leads to $CV=1$). These observations suggest that partial reset controls the bursting behaviour of the neuron.

These effects are the basis of an analytical model which predicts the effect of bursting on the *CV* and the variance $Var(N)$ of the number N of spikes counted in a given time interval. A core hypothesis in this model is that partial reset modifies the properties of a neuron in such a way that a burst is produced each time a single spike would otherwise be fired with total reset. Bursts are therefore supposed to be added to an underlying distribution of rather regularly spaced spikes. The numerical predictions of this model are overall consistent with results from simulations. However, the interspike interval histograms produced by

simulations do not show the bimodal distribution typical of bursting. Instead, the data are more consistent with a temporal clustering model in which a *distribution* of short interspike intervals is added to a distribution of long interspike intervals. Therefore, we will refer to temporal clusters of spikes rather than burst of spikes.

Clusters of spikes can be seen as multiple responses to favourable input events. Therefore, partial reset should increase the gain of a neuron. Simulations confirm that, for identical input conditions, partial reset increases the firing rate of the neuron. This increase is in good agreement with the number of spikes per cluster that is predicted by $CV(T)$ of $Var(N)$, according to the theoretical model. These results suggest that neurons with highly irregular firing are likely to have also a high-gain transfer function.

The paper is organised as follows. In section 2 we describe the model of neuron. In section 3, we describe the simulation procedure and give results of simulations under various reset and input conditions. In section 4, we present the temporal clustering models of the effect of partial reset. In section 5, we discuss the biological grounding of partial reset, its consequences on the neuronal function and compare our model to other models of the production of irregular spike trains. In section 6, we conclude.

2. Simulation of the Extended LIF Model of a Neuron

2.1 Summary of the model

The neuron model used in this investigation is an extended version of the standard Leaky Integrate-and-Fire (LIF) neuron [Harmon, 1961; Bugmann, 1991]. Apart from the feature of partial reset of the capacitor, described in section 2.4, the three other basic differences with the LIF are:

1) Input spikes do not cause a simple step-like increase in membrane potential as in [Softky and Koch, 1993] but initiate an excitatory post-synaptic current (PSC) extended in time and modelled by an alpha function (section 2.2). This function allows to reproduce qualitatively the current pulse widening effect of dendritic propagation [see e.g. Stratford et al., 1989]. The main advantage of this feature is that temporal effects associated with synaptic inputs at various electrotonic distances of the soma of the same neuron can be simulated. Our PSC's have the same functions as the postsynaptic responses (PSR) used to realise motion detectors with realistic response properties in [Christodoulou et al., 1992]. With the standard LIF model, all inputs are at the same electrotonic distance from the soma [Bugmann, 1991].

2) Successive PSC on the same synapse do not integrate temporally but saturate at a maximum value (see figure 1). However, PSCs from different synapses are integrated in the soma (the RC circuit of standard LIFs'). Saturating synapses are biologically plausible and allow neurons to operate as coincidence detectors despite long membrane time constants [Bugmann, 1992].

3) Synapses have probabilistic transmission properties. An input spikes generates a PSC with a probability P_t . This is based on physiological observations and gives interesting decaying memory properties to self-excitatory networks of spiking neurons [Bugmann and Taylor, 1995].

These three features extend the functionality of the LIF neuron but also affect the irregularity of the spike trains to various degrees. In this paper we show results of an investigation into the role of partial reset. The role of synaptic location is briefly described in section 3.5. The influence of other features is discussed briefly in section 5.

The neuron model is simulated on a PC-486 using the CORTEX-PRO software. In this simulator, wires linking neurons can have active properties. We have defined neurons to be simple leaky integrators (section 2.3) and the wires linking neurons to simulate the synapses and the dendritic propagation. They produce the PSCs extended in time and have probabilistic transmission properties (section 2.2). Such a wire reproduces in a simplified way some of the properties of the synapse and the dendritic propagation.

2.2 Saturating probabilistic synapses and dendritic propagation

A wire receives spikes from its input neuron and, for each spike, produces an internal alpha function PSC* contributing to the total postsynaptic current PSC:

$$PSC_{ij}^*(t_k) = E_{ij} \frac{t - t_{ok} - t_d}{T_{max,ij}} e^{-\frac{t - t_{ok} - t_d}{T_{max,ij} + 1}} \quad [1]$$

where t_{ok} is the time at which the input spike k has occurred and t_d is a propagation delay. In our simulations, t_d is set to 1 ms. The maximum amplitude of the PSC is equal to E_{ij} . It has the units of a current, but due to the simplifications described in section 2.3, we can think of it as a number of mV. The time course of the PSC is determined by the value of $T_{max,ij}$. By

selecting different values of $T_{max,ij}$ for each synapse, inputs at different electrotonic distances can be simulated. PSC with long time courses represent inputs on distant synapses.

In order to implement the saturating mechanism [Bugmann, 1992], the values PSC^* due to past input spikes are compared. The largest value becomes the actual $PSC_{ij}(t)$:

$$PSC_{ij}(t) = \max(PSC_{ij}^*(t_k)) \text{ for } k = 1 \text{ to } k_{max} \quad [2]$$

Where the index j is the identity of the input neuron sending the spikes to the synapse. To reduce the computation time, a limited number k_{max} of past input spikes is considered. However, if k_{max} is too small and a burst of input spikes has just occurred, the value of the tail of the older PSCs' may be lost before the new PSCs' have risen to a similar value. This causes discontinuities in the time course of $PSC_{ij}(t)$. In practice we have found that this problem can be avoided by using $k_{max} = 10$, i.e. storing the arrival time of the latest 10 spikes.

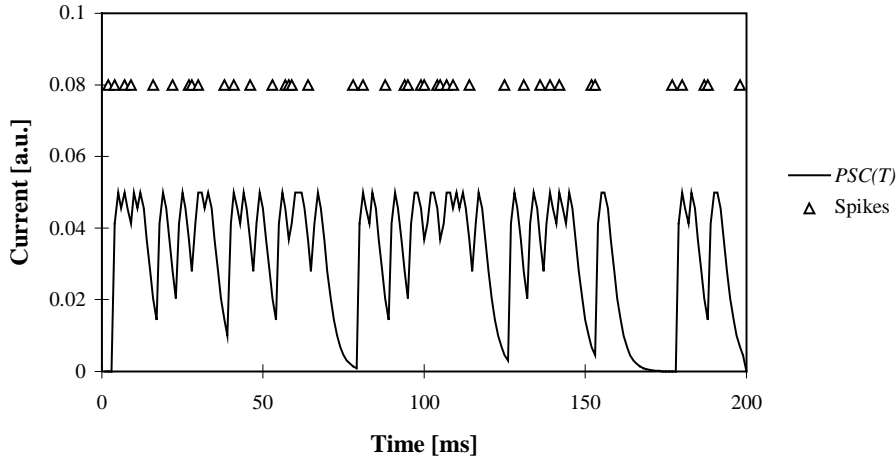


Figure 1: PSCs produced by a saturating synapse in our model, in response to input spikes indicated by triangles in the upper half of the figure. Input frequency $F_{in} = 173$ Hz, $T_{max} = 2$ ms, $E_{ij} = 0.05$.

In order to account for the probabilistic nature of the synaptic transmission (see references in [Bugmann and Taylor, 1995]), input spikes have a probability P_t of producing PSC*s'. An implementation using pRAM neurons is described in [Christodoulou et al., 1992]. In this paper we use $P_t = 1$.

2.3 Leaky integrator

The currents produced by the "dendro-synaptic" wires described above flow into a classic LIF neuron [Harmon, 1961; Bugmann, 1991]. It comprises a capacitor C in parallel with a leak resistor R . This system is characterised by a time constant $\tau = RC$. In our simulations we use $\tau = 10$ ms, which is an accepted value for cortical neurons (for instance, [Softky and Koch, 1993] use $\tau = 13$ ms). To reduce the simulation time on a PC, we use relatively large integration time steps $\Delta t = 1$ ms. Therefore, we must make clear in which order the operations are done: At each time step, the currents $PSC_{ij}(t)$ are first calculated based on the outputs of the inputs up to time $t-1$. Then potential V_i of the capacitor decays to V_i^* :

$$V_i^*(t) = V_i(t-1) \exp(-\Delta t / \tau_i). \quad [3]$$

Note that there is no explicit modelling of a capacitor and a leakage resistor. Then the sum of the potential increases due to the currents $PSC_{ij}(t)$ flowing into the capacitor is added to the potential:

$$V_i(t) = V_i^*(t) + \frac{\Delta t}{C} \sum_{j=1}^N PSC_{ij}(t) \quad [4].$$

Where N is the number of inputs to the neuron. Note that in this formulation, the input current is implicitly assumed to be constant during the time step. For simplicity we use $\Delta t = C = 1$. Therefore, the effect of a current $PSC_{ij}(t)$ is to increase the potential of the capacitor by a quantity $PSC_{ij}(t)$. We assume that this is measured in mV.

The actual synaptic weight W_{ij} is the average number of charges injected into the neuron for each input spike. Due to the saturation mechanism, this is dependent on the frequency of input spikes. In the case of low input frequencies, where saturation effects can be neglected, the synaptic weight W_{ij} can be approximated by the time-integral of $PSC_{ij}^*(t_k)$ which gives:

$$W_{ij} = E_{ij} * T_{max,ij} \quad [5]$$

In practice however, saturation effects are almost never negligible and synaptic weights can only be deduced from the actual synaptic currents measured on a step-by-step basis.

2.4 Firing, partial reset and refractory time

If the potential $V_i(t)$ exceeds a threshold V_{th} (we use $V_{th} = 15$ mV), a spike is produced (setting the output of the neuron to 1) and the potential is reset to

$$V_i(t) = \beta V_i^*(t), \text{ with } 0 < \beta < 1. \quad [6]$$

Where $V_i^*(t)$ is the potential at the moment of the comparison with V_{th} , just before the spike is initiated. When $\beta = 0$, the reset is total. When $\beta = 1$, there is no reset. A form of partial reset realised by subtracting a fixed potential difference after each spike was described by [Shigematsu et al., 1992].

Usually LIF neurons comprise a refractory time which has been modelled in various ways. For instance, the recharging of the capacitor can be prevented during a time Tr after the initiation of a spike [Bugmann, 1991] or the firing of a spike can be prevented during that time [Christodoulou et al, 1992]. To these forms of absolute refractory time one can add a relative refractory period by temporarily increasing the threshold after a spike [Harmon, 1961]. In our model, we use only an absolute refractory following a scheme similar to the one used in [Christodoulou et al, 1992]: The dendritic currents continue to flow into the capacitor after a spike, but the potential is simply not compared with V_{th} during the Tr time-steps following a spike. We have used $Tr = 1$, which results in a minimum delay of 2 time-steps between spikes (even with no explicit refractory time, there is at least one time-step between spikes).

2.5 Simulation of the inputs

The network used for the simulations comprises a single output neuron receiving inputs from $N = 50$ input neurons, via the "dendro-synaptic" wires described above. The input neurons are simple sources of independent random spike trains characterised by a probability P_{in} of

observing a spike at each time step. The inputs have is no explicit refractory time. In the remaining of the paper we will use the frequency equivalent of P_{in} : $F_{in} = P_{in}/1\text{ms}$.

3. Results

3.1 Simulation procedure

The main aim of these simulations was to obtain $CV(T)$ curves similar to those reported in the figure 9 of [Softky and Koch, 1993]. For that purpose, some of the parameters of the simulations were fixed and some were adjusted by hand until a satisfactory $CV(T)$ curve was obtained. Our criteria was: the largest value of $CV(T)$ should be close to 1 and $CV(T)$ for $T=10$ ms should be close to 0.8. The fixed parameters were: Range of input frequencies identical to the range of output frequencies, i.e. 0-400Hz; Threshold $V_{th} = 15$ mV; Membrane time constant $\tau = 10$ ms; Number of input $n = 50$. The adjustable parameters were: Time course of the PSCs determined by $T_{max,ij}$; Synaptic weights E_{ij} ; Reset parameter β ; Mode of production of the average input current.

We have used two values of $T_{max,ij}$. A short value of $T_{max,ij} = 2$ ms was taken to be representative of the time course of postsynaptic currents produced at proximal synapses. A long values of 20 ms was taken to represent distant inputs. It led to EPSPs reaching their maximum at approximately 50 ms. This is probably a not too bad approximation of results obtained with a more detailed model [Stratford et al., 1989].

The average input current is varied to produce output spike trains with various average interspike intervals T . This can be done in two ways: The input current can be varied by changing the frequency of the input neurons or by changing the number of active input neurons, or both. It is known that the response of neurons gradually decreases the more the stimulus differs from the optimal stimulus. In most of the simulations presented here we have assumed that the stimuli of the *input* neurons became progressively less optimal. This is simulated by a variation of the frequency of the inputs while keeping their number constant. All results have been produced under this condition. One additional set of simulation was done with a high input firing rate but with a variable number of inputs, to compare the transfer functions obtained with both ways of simulating input current variations (section 3.4).

The synaptic weights were set such that a reasonable range of output frequency could be scanned by varying the input frequencies in the pre-set range. With $T_{max,ij} = 20$ ms we used $E_{ij} = 0.029$. With $T_{max,ij} = 2$ ms we used $E_{ij} = 0.05$. In this later case, each input spike causes an increase of the membrane potential of typically 0.16 mV (observed approximately 8ms after the input time, due to the temporal integration of the tail of the *PSC*), which is in the range of biological values of EPSPs [Mason et al., 1991].

Finally, we have tried several values of β in order to obtain curves of $CV(T)$ similar to those recorded in cortical neurons. In following sections we present mainly detailed results for proximal synapses ($T_{max} = 2\text{ms}$). The results for distal synapses are mentioned in section 3.5 but detailed graphs are not shown.

Simulation times are typically 20000 time steps. The output spikes are used to calculate the coefficient of variation CV , average interspike interval T , distribution of interspike intervals (ISI) and spike counting statistics comprising the mean number N of spikes in a given time window, and the variance $Var(N)$ of that number.

3.2 Effect of partial reset on the irregularity of spike trains

Figure 2 illustrates the effects of partial reset on the time course of the membrane potential of the neuron. When the potential is reset to $\beta=0.98$ of the pre-spike potential, the neuron shows a clear bursting behaviour. In the case $\beta=0.0$, denoting full reset, one observes the standard results with such a model, rather regular firing and small values of CV [Softky and Koch, 1993]. In the case $\beta=0.91$, the firing looks random.

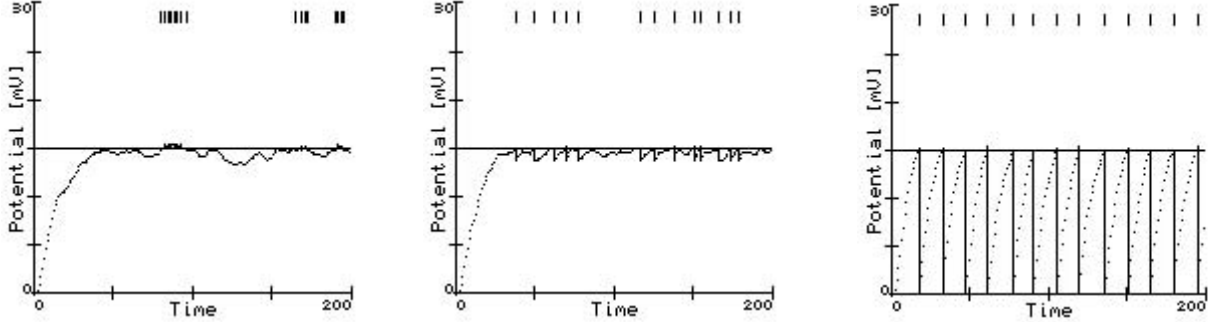


Figure 2. Potential of the capacitor during the first 200 ms of the simulation. The timing of the output spikes is shown at the top of the figures. **Left:** Reset to 98% of the potential before spiking, **Middle:** Reset to 91% of the potential before spiking. **Right** With total reset after spiking. Simulation conditions: Average interspike interval is 15 ms. (For 98%: $F_{in} = 161$ Hz; for 91%: $F_{in} = 179$ Hz and for 0%: $F_{in} = 280$ Hz). Other parameters: $E_{ij} = 0.05$, $T_{max} = 2$ ms (proximal inputs), Decay time constant $RC = 10$ ms, 50 excitatory inputs.

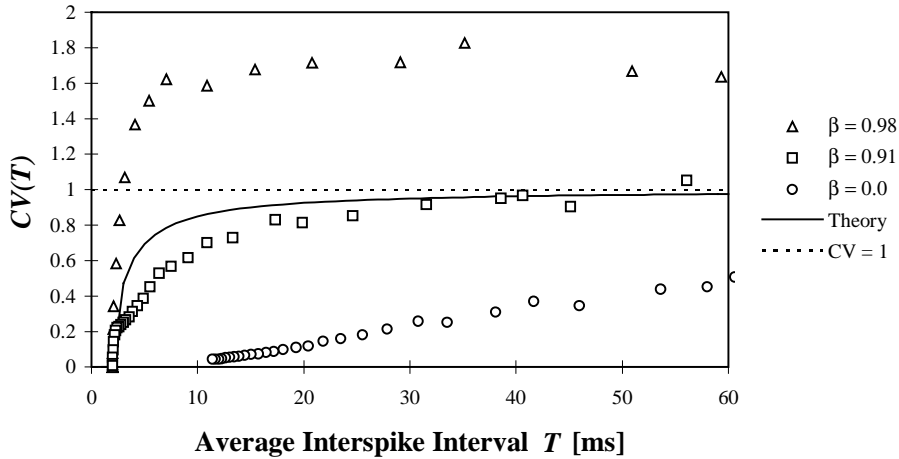


Figure 3. $CV(T)$ curves obtained with proximal synapses, for the indicated values of the reset parameter β . The full line shows the theoretical curve in the case of random spike trains: $CV(T) = \sqrt{\sigma^2(T)/T^2} = \sqrt{(T - Tr)/T}$ (see Appendix A.1). We used a refractory time $Tr = 2$ ms. Simulation conditions as in figure 2, except that input frequencies were scanned from 150 Hz to 400 Hz.

Figure 3 shows that bursting results in high values of CV and that regular firing causes low values of CV. Values in the physiological range, as measured by [Softky et al, 1993], can be

obtained with a partial reset to 91% of the pre-spike potential. In this case, the $CV(T)$ curve fits relatively well with the theoretical approximation, valid for small N , for spikes produced by a Poisson process with refractory time.

With $T_{max,ij} = 2\text{ms}$, the saturation effect in the neuron model should become noticeable for input frequencies approaching and exceeding 400 Hz. Compared to simulations done with a simple LIF model without synaptic saturation, where the curve for $\beta=0.91$ fits almost exactly with the theoretical curve [Bugmann et al., 1995], we see here a downward deviation, especially at high frequency. This is probably due to the reduced fluctuations in the saturated current.

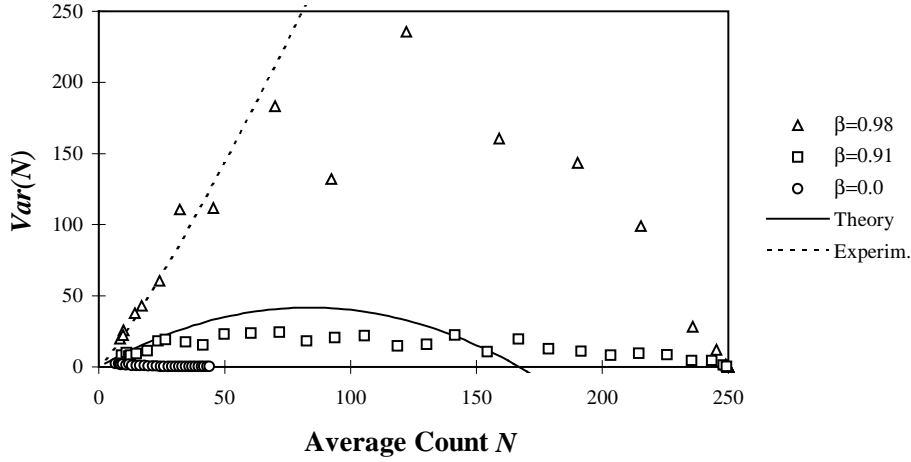


Figure 4. Variance $Var(N)$ of the number N of spikes counted in 500 ms for the indicated values of the reset parameter β . The x-axis represents the average number N of spikes produced in a 500ms time-window w . The duration of the simulated spike trains is 20000ms. The y-axis represents the variance of the average number of spikes N calculated over the 40 non-overlapping samples taken from a spike train. The dotted line represents the expression $Var(n) = A * N - B$, with $A = 1.6$ and $B = 1.15$, found to fit data in cortical neurons [Dean, 1981]. The continuous line is the theoretical approximation in the limit of small values of N for a random spike train: $Var(N) = N - N^2(1 + 2Tr)/w$, where $Tr (= 1)$ is the refractory time (see appendix B2). Simulation conditions as in figure 3.

Figure 4 shows that irregularities similar to the physiological values, as measured by $Var(N)$ [Dean, 1981] can be obtained with a value of β somewhere near to 0.98. The data used by [Dean, 1981] were restricted to $T < 30\text{ms}$, so only the lower part of the curves must be considered in figure 4. This correspondence suggests a possible mild bursting behaviour in neurons recorded by [Dean, 1981].

In the case $\beta=0.91$, the counting statistics fits relatively well with the theoretical approximation, valid for small N , for spikes produced by a Poisson process with refractory time.

3.3 Effects of partial reset on the interspike interval distribution

The results shown so far suggest that partial reset allows to control the statistical properties of spike trains in such a way it produces a continuous transition between bursting and regular firing, with an intermediate stage where the firing is apparently random. Is this stage characterised by a values of CV near to one, because of a true random firing or because of a fortunate combination of regular firing and mild bursting ? To address this question, we have observed the distribution of interspike intervals.

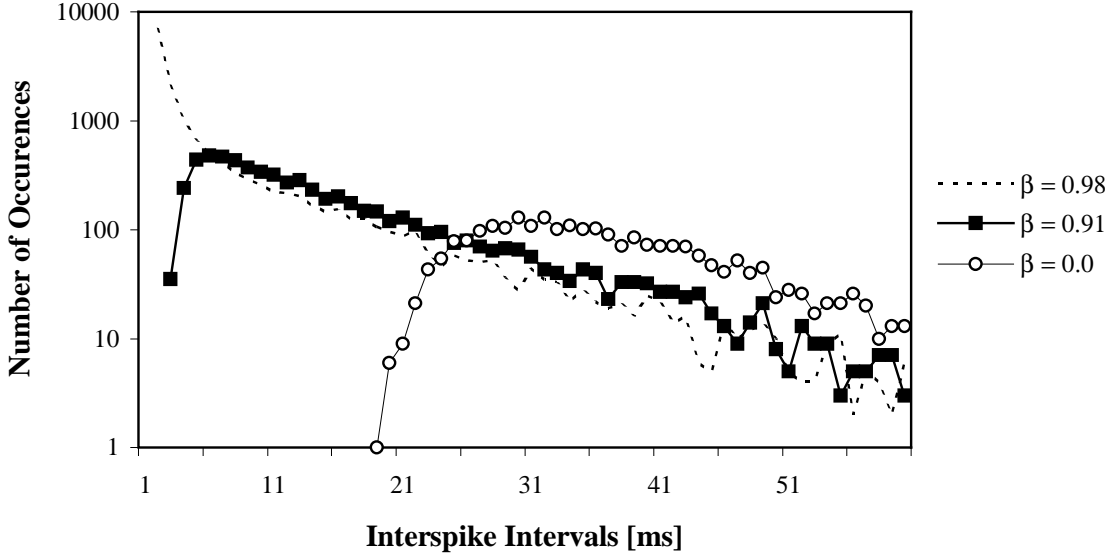


Figure 5. Histogram of number of intervals of indicated durations counted during 100000 ms. The vertical scale is truncated to enhance the curve for $\beta = 0$. With increasing value of β , the number of long interspike intervals is reduced. Simulations were done with proximal synapses and all parameters fixed except for β . ($T_{max} = 2\text{ms}$, $E_{ij} = 0.05$, $F_{in} = 173.5\text{ Hz}$, 50 inputs, corresponding to a current of 1.46 in figure 6). The total number of spikes produced for $\beta = 0.98$, 0.91 and 0.0 was respectively 15350, 6421 and 2591, corresponding to firing frequencies of 153 Hz, 64Hz and 26Hz respectively. The values of CV are: 0.32, 0.75 and 1.37. The values of $Var(N)$ are 1.91, 14.6 and 145.6, measured over non-overlapping time windows lasting 500ms.

The curves in figure 5 were produced with fixed input conditions for 3 values of the reset parameter β . We have plotted the number of intervals in each class and not the distribution, as is usually done. The curve for the case $\beta=0.91$ shows an exponential decay, a behaviour usually taken as indicating a Poisson process. The main difference between the curves for $\beta=0.91$ and $\beta=0.98$ is a huge increase of short intervals in the case $\beta=0.98$. The number of long intervals is almost unchanged. Comparing the curves for $\beta=0.91$ and $\beta=0.0$, we see that partial reset has added short intervals and removed some long intervals.

These observations can be explained using the clustering model analysed in section 4. The clustering model is based on the hypothesis that partial reset replaces single spikes that would normally be produced when total rest is used, by clusters containing γ spikes fired with close intervals. This has the effect of reducing the duration of long intervals and to create short intervals in the distribution.

3.4 Effect of partial reset on the gain of a neuron

The gain of a neuron is essentially given by the slope of its transfer function for input currents above threshold. For a very steep slope, the neuron can operate like a logical gate, with two states. This is the high gain limit. Clustering is a way to increase the gain, because every spike is now replaced by γ spikes. Figure 6 confirms that partial reset is a very effective method of increasing the gain of the neuron.

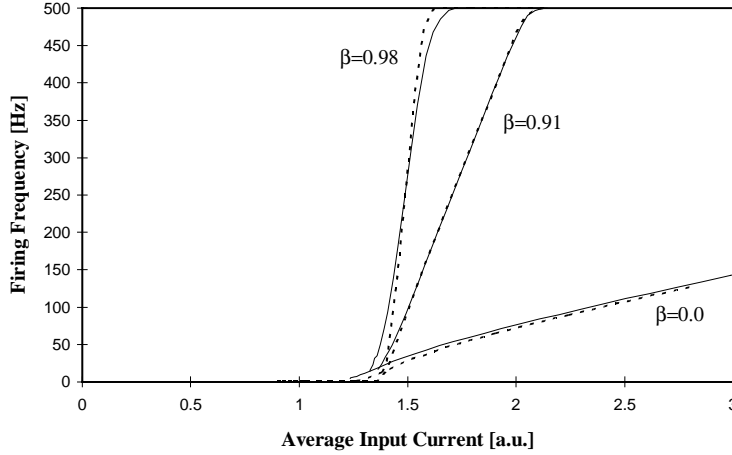


Figure 6 Dependence of the output firing frequency on the average input current for an extended LIF neuron model with proximal synapses. **Full lines:** The average input current is scanned by progressively increasing the firing frequency of the 50 inputs from 150 Hz to 400 Hz. **Dotted lines:** The average current is scanned by varying the number of active inputs having all a firing frequency of 400 Hz. The average input current is measured during simulation. Other parameters: $T_{max} = 2$ ms, $E_{ij} = 0.05$.

We may note in figure 6 that the output frequency does not depend much on how the input current is produced, except for small output frequencies where coincidence detection plays a crucial role [Bugmann, 1992]. For most of the curve, the average input current is a reasonably good input value for a transfer function.

As a consequence, if we assume that each input spike train is produced by a neuron coding for a component of a complex pattern, then the neuron in figure 6 would respond similarly to the presentation of an incomplete but clear pattern or to a complete pattern but with components not well recognised. In terms of pattern recognition, partial reset gives the neuron a less graded and more binary response. It does not modify the threshold, because partial reset has the same effect as a positive feedback.

3.5 Role of the dendritic location of the inputs.

Most of the simulations performed with proximal synapses ($T_{max} = 2$ ms) were also performed with distal synapses ($T_{max} = 20$ ms). These results are described in details in [Bugmann, 1995]. We summarise here some of the main features.

Concerning the simulation conditions, as the PSC* induced by an input spike lasts longer than for proximal inputs, a larger number of charges is injected into the capacitor for a same value of E_{ij} . To keep the range of input frequencies in relation with the range of output frequencies, the weights were decreased to $E_{ij} = 0.029$.

Concerning the effects of partial reset, obtaining irregularities in the target range, required using values of β very close to 1. Curves similar to those in figure 3 were obtained using $\beta = 0.99, 0.995$ and 0.998 . This showed that small variations in the value of β resulted in large variations of the values of CV . The same applies to the counting statistics. This makes the control of the irregularity of the spikes trains more difficult than with short PSCs'.

Concerning the transfer functions, in these three cases, the three transfer functions were perfectly binary, with a minute increase of input current leading to firing with maximal rate ($1/T_r$). As the synaptic saturation mechanism is used and the PSCs having a long duration, varying the input frequencies over the normal range 150-400Hz did almost not modify the input current.

We may note that with a fixed somatic reset parameter β , the displacement of input activity from distant to proximal synapses, leads to a more irregular firing. As a rule of thumb it is reasonable to assume that proximal inputs are involved when irregular firing is observed.

4 Modelling the effects of partial reset

4.1 Time dependent threshold and the clustering hypothesis

After partial reset, the potential of the membrane is βV_{th} . Thus the effective threshold for firing is $(1-\beta)V_{th}$. At that moment, a very small input current can cause the neuron to fire. However, if no inputs occurs, then the potential decays towards the resting potential and the effective threshold increases towards V_{th} . Partial reset can be seen as an initial charge set into the capacitor, which decays, as do other charges due to inputs. Therefore, even in the presence of inputs, the effective threshold increases with time after each output spike.

Due to this time dependence of the effective threshold, inputs occurring shortly after a spike are likely to cause the neuron to fire again. However, if effective inputs do not occur within 10-15ms (decay time), then the neuron operates again with its full threshold and produces rather long interspike intervals based on the temporal integration of a number of input spikes. This description suggests a very crude hypothesis: Partial reset is adding bursts to spike trains which otherwise would look very similar to those produced by a leaky integrator neuron with total reset.

In section 4.4 we will see that the shape of the interspike interval distributions is more consistent with a clustering model than with a strict bursting behaviour. One should therefore assume that partial reset causes some form of repetitive firing, which may take the form of bursts in extreme cases and simple "temporal clusters" of spikes in milder cases. For convenience however, the theoretical analysis is done here assuming strict bursting.

The question of how clusters are generated and how the number γ of spikes in a cluster is determined is not further addressed here. Experimental support for a clustering model of neuronal firing can be found in [Grüneis et al., 1989; 1990].

In section 4.2 we analyse the effect of clustering on the irregularity of spike trains and, in section 4.3, the effect of clustering on the gain of the neuron.

4.2 Effects of temporal clustering on the statistics of spike trains.

To quantify the effects of bursting on the statistical properties of spike trains we consider that, with total reset, the neuron would fire spikes according to the *underlying* distribution $P(k)$ of interspike intervals k . We assume that, due to partial reset, each spike normally produced according to the distribution $P(k)$ is replaced by a burst containing γ spikes. It is shown in the Appendices A and B that for low firing frequencies (small N or large T):

$$CV(T)_{Burst} \approx \sqrt{\gamma(CV(T)_{Underlying}^2 + 1) - \frac{2(\gamma-1)(1+Tr)}{T} - 1} \quad [7]$$

For an underlying Poisson process it is known that $CV(T) = 1$ and the expression [7] reduces to:

$$CV(T)_{Burst} \approx \sqrt{2\gamma - \frac{2(\gamma-1)(1+Tr)}{T} - 1} \quad [8]$$

A general expression for the variance $Var(N)$, valid for any underlying distribution of interspike intervals can be found in [Bair et al., 1994]. In our model of clustering, the expression of [Bair et al., 1994] would reduce to:

$$Var(N)_{Burst} \approx \gamma^2 Var(N')_{Underlying} \quad [9]$$

Where N' is the number of counts that the underlying process would produce. In the case of a Poisson process, $Var(N') = N'$ and with our model of bursting $N' = N/\gamma$. In this case, [9] becomes [10].

$$Var(N)_{Burst} \approx \gamma N \quad [10]$$

We may note that for $\gamma=1$, the expressions [8] and [10] reduce to those for spike trains produced by a pure Poisson process.

Strictly speaking, the above expressions do not apply to real spike trains because they have been developed assuming discrete time steps. However, in the low frequency limit, they may constitute a good approximation, and may allow a rapid assessment of the bursting behaviour of a recorded neuron, provided the values of CV or $Var(N)$ are related to bursting, and one has a good reason to assume a given interspike intervals distribution of the underlying process.

Consistency of the assumption of an underlying Poisson process:

In general values of $Var(N)/N$ or CV larger than 1 are taken as an indication for a bursting behaviour. If the underlying process is a Poisson process, then the value of γ can be calculated from $Var(N)/N$ using expression [10] as in [Gruneis et al, 1989] or from CV using expression [8]. As an example, let us apply these equations to the data from the neurons recorded by [Dean, 1981], one finds that these neurons may have been bursting with approximately $\gamma = 2.5$ spikes per burst. Analysing data recorded in cat, [Gruneis et al, 1989] found $\gamma = 1.95$ in an attentive state and $\gamma = 18.1$ in paradoxical sleep.

Let us apply expression [10] to the case $\beta=0.98$ in figure 3. For large values of T , CV saturates at approximately 1.6. From equation [8], this gives $\gamma = 1.9$. According to equation [10], this should lead to a variance with an initial slope of 1.9 in figure 4. This value would constitute an excellent fit to the data, and may provide evidence that the model "Poisson+cluster" is valid for values of $CV > 1$.

The case $\beta=0.98$ in figure 5 is more difficult to exploit because the firing rate is higher, which may invalidate the approximations made during the theoretical developments the equations. Nevertheless, applying [8] we find $\gamma = 1.63$. From the variance $Var(N)$ and the number of spikes counted in 500ms ($N=77.6$) and applying [10], one finds $\gamma = 1.88$. If one assumes that the case $\beta=0.91$ corresponds to a neuron firing a Poisson spike train, then γ can be estimated from the number of spikes per burst needed to explain the difference in firing rate between the case $\beta=0.98$ and the case $\beta=0.91$ (see caption of figure 5), one finds $\gamma = 2.39$. As the neuron does not really fire a Poisson spike trains in the case $\beta=0.91$, as indicated by $CV=0.75$, this last estimation of γ may not be reliable. So, again, there is a reasonable agreement between values of γ found assuming an underlying Poisson process.

Consistency of the assumption of a more regular underlying distribution:

The hypothesis that the underlying process is a Poisson process is not necessarily true and is difficult to verify experimentally. In our simulations and we have access to the initial distribution. We would like to verify that it is an *underlying* distribution in the sense that, when clustering is added to it, it reproduces the properties of the spike trains in the cases $\beta=0.91$ and $\beta=0.98$.

| β | γ_{CV} | γ_{Var} | γ_N |
|---------|---------------|----------------|------------|
| 0.91 | 2.73 | 2.76 | 2.48 |
| 0.98 | 4.64 | 8.73 | 5.92 |

Table 1. Values of γ found for two spike trains produced with $\beta=0.91$ and $\beta=0.98$. The calculations were done using the interspike interval distribution of the case $\beta=0.0$ as the underlying distribution. The value γ_{CV} is obtained using equation [7]. The value γ_{Var} is obtained using equation [9]. The value γ_N is obtained by dividing the number of spikes produced with $\beta=0.91$ or $\beta=0.98$ by the number of spikes produced with $\beta=0.0$, as indicated in the caption of figure 5.

Applying [7] to the data of figure 5, we find $\gamma=2.73$ for $\beta=0.91$ and $\gamma=4.64$ for $\beta=0.98$. The same exercise can be done using the counting statistics. Using [9] we find $\gamma=2.76$ for $\beta=0.91$ and $\gamma=8.73$ for $\beta=0.98$. Using the actual increase in numbers of fired spikes due to partial reset, as indicated in the caption of figure 5, we find $\gamma=2.48$ spikes per burst in the case $\beta=0.91$ and $\gamma=5.92$ in the case $\beta=0.98$. These values are summarised in table 1.

In the case $\beta=0.91$ there is a reasonable agreement between the theoretical values of γ calculated assuming the case $\beta=0.0$ as underlying distribution. In the case $\beta=0.98$, the agreement is not so good, but due to the high firing frequency, the theory is less accurate. A better prediction of γ by expression [8] may be due to its term taking into account high-frequency effects. Such a term is lacking in expression [9].

Estimating the size of clusters in simulated spike trains.

So far, there is no strong case for excluding any of the two models. We will see here that even by observing the actual spike trains it is difficult to make a clear decision. There have been suggestions on how to assess bursting [Bair et al., 1994] but for clustering, which is a more fuzzy concept, there is no accepted method.

For instance in figure 7, we may count any isolated spike or group of spikes as a cluster. One finds then that there are approximately $\gamma=2.48$ spikes per cluster. If one counts as clusters the groups of spikes separated by a "sufficiently large gap" (measured by eye) without spikes, one finds $\gamma=7.4$. Each value is consistent with one of the models of underlying distribution.

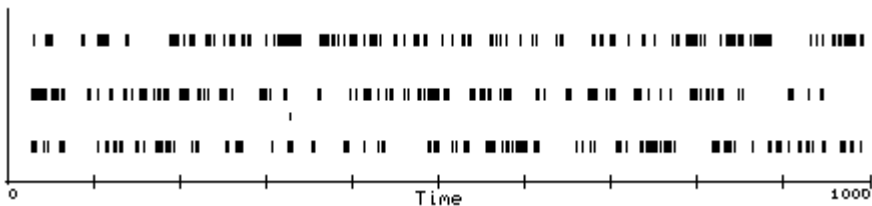


Figure 7. Examples of spike trains produced by the extended LIF neuron model during the 1000 initial simulation time-steps, for 3 run with different random number seeds used for the production of input spike trains. Simulation parameters identical to the case $\beta=0.98$ in figure 5.

We will see in the next section how the interspike interval distribution suggest that both approaches may be equivalent

4.3 Effects of temporal clustering on the interspike interval distribution

It is expected from the temporal clustering model that clustering reduces the duration of all intervals in the underlying distribution and adds a corresponding number of short intervals to the distribution. To assess if the reduction observed in the figure 8 is occurring in a proportion predicted by a simple bursting model we have first compared the curves for $\beta = 0.0$ and 0.91 . We have assumed an average interval of 9 ms for the spikes in bursts, slightly to the right of the peak in the curve for $\beta = 0.91$. By comparing the number of spikes produced with $\beta = 0.0$ and 0.91 (caption of figure 5) we estimate that there are $\gamma=2.5$ spikes per burst. In that case, bursting would reduce the average interspike intervals by $\tau=13.5$ ms (see Appendix A.2). Thereby, the peak at 30 ms in the $\beta = 0$ distribution should contribute to intervals of 16.5 ms in the $\beta = 0.91$ distribution. To test that hypothesis we have subtracted from the curve for $\beta = 0.91$ the curve for $\beta = 0.0$, shifted by 13 ms (only integer steps are possible with our data). The curve marked "cluster" in figure 8 shows that this operation is reasonably effective in cutting the tail of the curve for $\beta = 0.91$, leaving in principle only intervals between the spikes within bursts. Therefore, this curve could represent the distribution of intervals within clusters.

The same calculation can be done with the $\beta = 0.98$ curve. The interspike intervals in bursts is estimated to be 3ms, the number of spikes in a burst approximately 6, and the expected shift approximately $\tau=15$ ms. The subtraction of the shifted $\beta = 0.0$ curve leaves a narrow distribution peaked at an interval of 2 ms (not shown).

So, grossly speaking, the histograms of interspike intervals are compatible with a simple model of clustering where spikes produced according to an underlying distribution are replaced by a cluster of spike. Our theoretical model assumes regular intra-burst intervals, while the data suggest a distribution of intervals, but this is no fundamental difference.

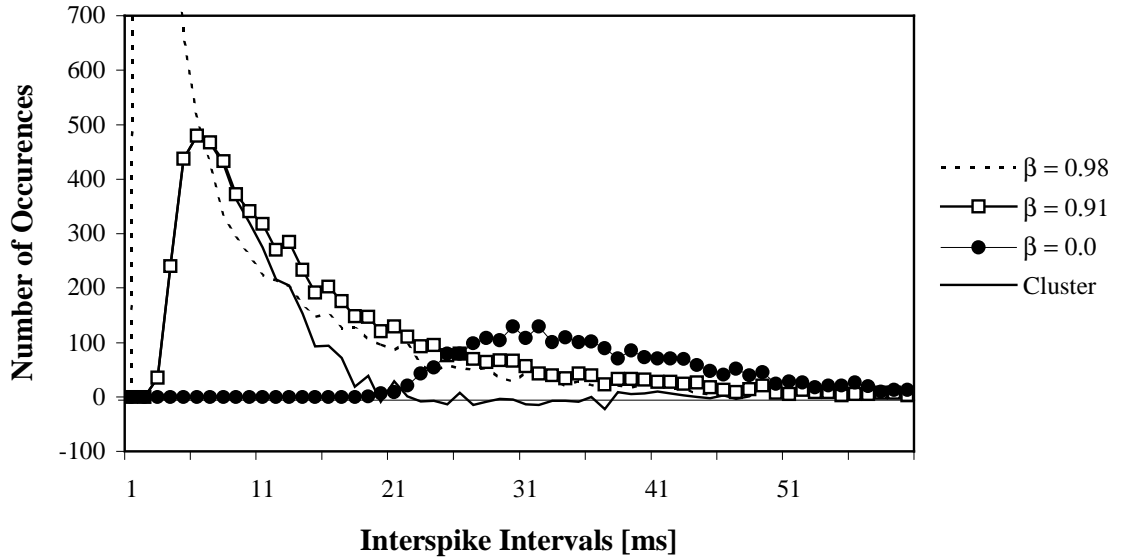


Figure 8. Histogram of number of intervals of indicated durations counted during 100000 ms. The vertical scale is cut to enhance the curve for $\beta = 0$. With increasing value of β , the number of long interspike intervals is reduced. Simulations were done with proximal synapses in the same conditions as in figure 5. The full line represents the $\beta = 0.91$ curves from which the $\beta = 0$ curve, shifted by 12 ms towards smaller times, is subtracted. According to our model, this represents the distribution of interspike intervals in clusters (or bursts).

However, the curve obtained with $\beta = 0.91$ curve shows an exponential decaying tail and is indistinguishable from a pure Poisson process with a refractory time. It must be concluded that the clustering process has to operate in such a way that, as β decreases, there is a wider and wider distribution of interspike intervals in the cluster. Thereby, for $\beta=0.91$ (in this model), the distribution of intervals between spikes within clusters does perfectly fill-in the missing short intervals in the slow distribution. As β decreases further, the number of spikes in clusters decreases and eventually disappear completely, leaving an unaltered slow distribution.

It is probably by such a process that partial reset can cause a continuous transition between bursting and regular firing, with an intermediate state of convincing random firing. Therefore, it is probably equivalent describe the curve for $\beta=0.98$ as resulting from the distribution for $\beta=0.0$ being augmented by clustering with $\gamma=5.9$ or as resulting from a Poisson distribution being augmented by clustering with $\gamma=1.63$.

4.4 Effect of clustering on the gain of the neuron.

When clustering takes place, the neuron produces more spikes in response to a given input. This increases its gain, as illustrated in figure 6.

The gain is the *slope* of the transfer function. If one knows the slope of the underlying transfer function, then one can exploit the measurement of γ to determine the new value of the gain. However, at present it is not possible to establish a direct link between irregular

firing and gain. Such a link would be useful for the assessment of the function of biological neurons from the statistical properties of their spike trains.

We may notice that partial reset results in the injection of a considerable charge $Q_r = C \cdot \beta \cdot V_{th}$ into the capacitor after each output spike. This may be approximately equivalent to a positive feedback increasing the effective input current, although this is not a random input. Unfortunately, there is no analytical expression for the firing frequency of our neuron model in dependence on the input current, so that this approach cannot be exploited further.

5. Discussion

5.1 Role of features of the model in controlling the irregularity of spike trains

The extended LIF model used here has several special features i) Partial reset ii) Probabilistic synapses, iii) Saturating synapses, iv) Postsynaptic currents extended in time (PSC),

Partial reset has a strong influence on the irregularity of the spike trains.

Probabilistic synapses have not been used in these simulations. They do probably not affect the irregularity directly. They reduce the frequency of effective input spikes [Christodoulou et al., 1995], and can increase CV by reducing the output firing frequency.

Synaptic saturation causes a reduction of CV , compared to a model with integration of successive PSCs [Christodoulou et al., 1995] or a model with step-like potential increase due to input spikes [Bugmann et al., 1995]. Synaptic saturation dampens the fluctuations of input firing rate and causes a more regular firing. Saturation mainly reduces CV at high input frequency, and for distal synapses.

Postsynaptic currents extended in time (PSC) used in this model have shown that, for a same firing frequency, the irregularity strongly depends on the location of the synapses providing the input current. With a similar value of β , distant inputs produce a more regular firing. With PSC's of long duration, the control of the irregularity is more difficult, because β has to be set in a very small range. It is not clear how a real neuron would set β to precise values like 0.998. It is therefore probable that slow PSCs do not generate large irregularities and that mainly proximal synapses are involved.

5.2 Biological justification of partial reset

It was made clear in the introduction that the main motivation for introducing partial reset was the rather technical problem of controlling the coefficient of variation of the interspike intervals. However, a purely biological justification of partial reset can also be attempted.

For instance, one may note that one of the effects of partial reset is that the membrane potential does not return to the resting potential while inputs are active (Figure 2). This is also observed in biological neurons and models of biological neurons [Mahowald and Douglas, 1991]. The degree of resetting is controlled by the repolarising Potassium current and it has been shown that this current can affect the irregularity of spike trains [Bell et al., 1995].

Another possible cause for the non-return to resting potential in biological neurons may be a decoupling between spike trigger zone and soma. This has been suggested by [Bras et al., 1987] who noted that the production of a spike at the axon hillock usually does not trigger the whole soma. Decoupling between the soma and the dendritic tree is an accepted idea (Although we did not find a reference to experimental data in support of this idea). One may possibly also have to assume a decoupling between axon hillock and soma. Such a decoupling would cause electrodes planted in the soma to record a partial reset while a total reset takes place at the axon hillock.

We may note that we obtain biologically realistic irregularities of spike trains by resetting the membrane to 91% of the potential. In a model of motion detection, we have used $\beta = 100\%$ to reproduce biological response curves [Christodoulou et al., 1992]. Experimental variance

curves $Var(N)$ can be obtained with β close to 98% (with proximal synapses, fig. 6). In the decoupling hypothesis, these results would suggest a strong decoupling between the axon hillock and the other parts of the soma. To account for this, compartmental models should comprise at least 3 compartments representing trigger zone, soma and dendrites.

The term "partial reset" has been used previously to indicate a decoupling between soma and dendrites [Christodoulou et al., 1992, 1994; Rospars and Lansky, 1993]. These models are designed in such a way that dendritic currents are not to be affected by a reset in the soma. However, the soma is completely reset by each output spike. In our model, the soma itself is partially reset.

Bursting is a common firing behaviour in cortical neurons, see e.g. [Bair et al., 1994], and it may play a role in neural coding [Parodi et al., 1995]. Bursting is a property of neurons based on the Hodgkin-Huxley equation [Carpenter, 1979], but their simulation is computationally intensive. It is interesting that, by adding the partial reset feature to simple LIF models, one can extend their capabilities into the bursting regime at a very small computational cost.

5.3 Comparison to other models

The problem of producing high-frequency irregular spike trains mentioned by [Softky and Koch, 1992, 1992] has generated three classes of models. One class relied on the dynamics of the neural network in which the neuron is embedded to increase the irregularity of the spike trains [Usher et al., 1994; Zipser et al., 1993]. A second class relied on inducing a random walk of the membrane potential by balancing excitatory and inhibitory inputs [Shadlen and Newsome., 1994]. Some authors use a similar mechanism but prefer to analyse its operation in terms of fluctuation or coincidence detection [Tsodyks and Sejnowski, 1995; Bell et al., 1995]. A third class exploits slow variations in input current [Rospars and Lansky, 1993; Lansky and Rospars, 1995]. Many models actually use combinations of these mechanisms.

An example of a model based on network dynamics can be found in [Usher et al., 1994], where a LIF neuron is imbedded in a cluster of neurons providing short range excitatory feedback and intermediate range inhibitory feedback. During a certain time, excitation is predominant and causes firing at a higher rate. Later inhibition is dominant and the neuron fires at a low rate. This succession of active and silent periods modifies the shape of the interspike interval distribution (ISI) and can produce spike trains with $CV > 1$. Due to the fact that network dynamics is chaotic, the tail of the ISI is characterised by a power-law decay. This feature should allow to verify this model experimentally. [Usher et al., 1994] have not attempted to simulate neurons with firing rates larger than 50 Hz, so that it is not certain yet that their model constitutes a solution to the high frequency irregularity problem [Softky and Koch, 1993].

In our model, the clustering process modifies also the shape of the ISI, but is controlled by the random stream of input spikes. Therefore, the tail of the distribution decays exponentially, as shown in figure 5 (A log-log plot would show a strong downward bending of the tail). So, the decay mode may be able to distinguish the two models.

A form of partial reset was proposed by [Wilbur and Rinzel, 1983] who needed such a mechanism to reproduce the ISI or biological spike trains with a simple LIF model. Later, [Lansky and Musila, 1991] investigated the effects of fluctuations of the reset potential βV_{th} . A characteristic of partial reset is that it has the same effects as a time dependent threshold, where the values of the effective threshold increases with time from a small value towards the nominal value. We may note that some model neurons implement the refractory time in form

of a decreasing threshold, where just after firing, the threshold has an initial high value, and then decreases towards the nominal value. The fast time constant of that decay does not make it incompatible with the slow increase following partial reset.

Recently, a form of partial reset was used in a way such it does not lead to a time-dependent threshold. In the model of [Tsodyks and Sejnowski, 1995] a neuron is imbedded in a recurrent network and receives excitatory and inhibitory inputs from this network and a bias input representing external input, e.g. sensory information. The bias current has an amplitude such that, after partial reset, the average value of the potential increases very slowly, even without recurrent input. So, in this model, the combination of partial reset and bias input result essentially in a smaller and relatively constant threshold.

In this situation, the neuron relies on favourable sequence of excitatory and inhibitory inputs for its potential to reach the firing threshold again. [Tsodyks and Sejnowski, 1995] suggest that their model achieves high irregularities, i.e. CV near to one, because it is driven by fluctuations in input current. However, as a consequence of the bias input, when an excitatory input has raised the potential by a certain amount, the potential stays at this new value and goes on rising slowly. Inversely, an inhibitory input decreases the potential by a certain amount. The potential then continues to rise slowly from this new value. As a result of successive excitatory and inhibitory inputs, the membrane potential undergoes probably a random walk which can lead to irregular firing [Shadlen and Newsome, 1994].

In principle, a random walk cannot lead to values of CV larger than one, but this may be achieved in the model of [Tsodyks and Sejnowski, 1995] due to the network dynamics.

Our model can probably be analysed in terms of random-walk model, possibly exploiting tools developed in [Ricciardi and Sacerdote, 1979]. One of the two main particularities of our model is that the random walk is asymmetrical, increases being due to synaptic inputs and decreases being due to decay. The other particularity is the time-dependent effective threshold.

We may also note other differences with some random-walk models: For instance, in contrast to [Lansky and Musila, 1991], we use only excitatory inputs to produce high values of CV , with a non-zero refractory period. In [Tsodyks and Sejnowski, 1995] the average input current is restricted to be close to the threshold current (minimum current needed to fire the neuron) while we scan a range of average input currents. In [Shadlen and Newsome, 1994] the random walk is not allowed to produce values of the potential below the initial potential while we do not make such a restriction.

In the 2-point model of [Rosparis and Lansky, 1993], high values of CV are obtained by isolating dendritic currents from the (total) reset process in the soma. After a spike has been produced by a high input current, it is likely that the current be still high so that a second spike is produced within a short interval. The same principle is used in [Christodoulou et al., 1994] and allows to produce burst or clusters of spikes.

In our model we are also preserving dendritic currents but, in the results presented here with short $PSCs$, this is not the cause of the clustering. As evidence, we have obtained almost the same curves as in figure 3 with a simple LIF model, without $PSCs$, where input spikes cause a stepwise increase of the membrane potential [Bugmann et al., 1995]. In our model partial reset is the crucial mechanism whereby each output spike facilitates subsequent firing during a short time. It does so by leaving a considerable positive charge in the capacitor.

Thus the clustering observed here is not based on a memory of input currents but is a consequence of a positive feedback action caused by partial reset.

5.4 Neuronal function

It has been proposed that modelling the irregularity of biological spike trains would help to understand the function of biological neurons, for instance in terms of number of inputs, integration time constant, etc. [Stein, 1997; Bugmann, 1990]. However, if we consider the recent results by [Usher et al, 1994; Zipser et al., 1993] showing that the network dynamics can increase the irregularity of spike trains, it has become clear that the observed irregularities can be a combined effect of intrinsic mechanisms, as those described here, and of extrinsic network effects. Therefore, modelling the production of irregular spike trains with single neurons mechanisms alone or with network effects alone, does not allow to draw very strong conclusions on neuronal, or network, functions. One may have to introduce additional constraints in simulations, for instance by giving more attention to the computation performed by simulated systems. Ultimately, using realistic neuron models in real tasks like robot control.

However, a common feature of our work and the one of [Usher et al, 1994] is the need to increase the gain of the neuron to increase its irregularity. In past publications [Bugmann, 1991, 1992] we have shown that decision functions such as AND functions or multiplication caused a loss in signal level. The partial reset mechanism proposed here can compensate for this loss, and the positive feedback in [Usher et al, 1994] probably also. Neurons with less selective functions, such as summation, do not need a high gain. It is therefore tempting to suggest that a high firing irregularity is linked to a function with high selectivity.

6. Conclusion

The 3 main contributions of this report are: i) A new model of neuron is described, ii) An effective and simple mechanism for controlling the irregularity of spike trains is demonstrated and iii) A link is suggested between firing irregularity and neuronal function.

One of the features of the model, partial reset, is a powerful tool to control the irregularity of the spike trains and the gain of the transfer function of the neuron.

Partial reset may reflect a weak repolarisation or a partial decoupling between trigger zone and soma. In any case, it is a biologically grounded mechanism and a computationally simple way to increase the realism of the firing behaviour of a simple leaky integrator neuron model.

Other mechanisms have also been proposed for the production of irregular spike trains, but have not been used to reproduce the $CV(T)$ curves which were reported by [Softky and Koch, 1993]. So, it is difficult to assess how crucial partial reset is for neural modelling. For instance, high irregularities could also reflect fluctuations in firing rate induced by network dynamics [Usher et al, 1994; Zipser et al., 1993]. Therefore, the irregularity problem has not yet taught us something definitive about the neuronal function.

In order to learn more on the functions of biological neurons or biological neural networks, additional constraints must be introduced into modelling, for instance by specifying the information *processing* task. Along these lines, applications to bio-control problems may prove doubly rewarding, as applications, and as sources of new insight into brain functions.

Nevertheless, intrinsic and extrinsic sources of high irregularity result both in a higher gain of the neuronal transfer function, via internal or external feedback. It would therefore be

interesting to obtain an experimental confirmation that gain, or a related measure such as the selectivity to input patterns, is related to the irregularity of the spike trains.

Acknowledgements

We are thankful to Christian Lehmann, Mike Denham and Raju Bapi for very helpful comment on earlier versions of this manuscript and John G Taylor and Chris Christodoulou for stimulating discussions.

7. References

Bair W., Koch C., Newsome W. and Britten K. (1994) "Power spectrum analysis of bursting cells in area MT in the behaving monkey", *The Journal of Neuroscience*, 14, pp. 2870-2892.

Bell A.J., Mainen Z.F., Tsodyks M. and Sejnowski T.J. (1995) "Balancing conductances may explain irregular cortical spiking", Technical Report no INC-9502, February 1995, Institute for Neural computation, UCSD, San Diego, CA 92093-0523, USA.

Bras H., Gogan P. and Tyc-Dumont S. (1987) "The mammalian central neuron is a complex computing device", *Proc IEEE 1st Intl. Conf. on Neural Networks*, San Diego, California, vol. IV, pp. 123-126.

Bugmann, G. (1990) "Irregularity of natural spike trains simulated by an integrate-and-fire neuron", *Extended Abstracts, 3rd Int. Symp. on Bioelectronic and Molecular Electronic Devices*, Kobe (edited by R & D Association for Future Electron Devices, Japan), 105-106

Bugmann, G. (1991) "Summation and multiplication: two distinct operation domains of leaky integrate-and-fire neurons", *Network*, 2, 489-509.

Bugmann, G. (1992) "Multiplying with neurons: Compensation for irregular input spike trains by using time dependent synaptic efficiencies", *Biological Cybernetics*, 68, 87-92.

Bugmann G. and Taylor J.G. (1994) "A top-down model for neuronal synchronisation", *Research Report NRG-94-02*, October 1994, School of Computing, University of Plymouth, Plymouth PL4 8AA, United Kingdom.

Bugmann G. (1995) "Controlling the irregularity of spike trains", *Research Report NRG-95-04*, July 1995, School of Computing, University of Plymouth, Plymouth PL4 8AA, United Kingdom.

Bugmann G. and Taylor J.G. (1995) "A stochastic short-term memory using a pRAM neuron and its potential applications", in Beale R. and Plumbley M.D. (eds) "Recent advances in neural networks", to be published by Prentice Hall.

Bugmann G. Christodoulou C. and Taylor J.G. (1995) "The highly irregular firing of cortical cells is consistent with temporal integration of random EPSPs", submitted

Carpenter G.A. (1979) "Bursting phenomena in excitable membranes", *SIAM J. Appl. Math.*, 36, pp. 334-372.

- Christodoulou, C., Bugmann, G., Taylor, J.G. and Clarkson, T. (1992) "An extension to the temporal noisy-leaky integrator neuron and its potential applications", Proc. IJCNN'92 (Beijing), Vol III, 165-170.
- Christodoulou C., Clarkson T., Bugmann G. and Taylor J.G. (1994) "Modelling of the high firing variability of real cortical neurons with the temporal noisy-leaky integrator neuron model", Proc. IEEE Int. Conf. on Neural Networks (ICNN'94) part of the World Congress on Computational Intelligence (WCCI'94), Orlando, Florida, USA, 2239-2244.
- Dean A.F. (1981) "The variability of discharge of simple cell in the cat striate cortex", Exp. Brain Res., 44, 437-440.
- Gruneis F., Nakao M., Yamamoto M., and Nakahama H. (1989) "An interpretation of 1/f fluctuations in neuronal spike trains during dream sleep", Biol. Cybern., 60, 161-169.
- Gruneis F., Nakao M., and Yamamoto M. (1990) "Counting statistics of 1/f fluctuations in neuronal spike trains", Biol. Cybern., 62, 407-413.
- Harmon L.D. (1961) "Studies with artificial neurons, I: Properties and functions of an artificial neuron", Kybernetik, 1,789-101.
- Lansky P. and Musila M. (1991) "Variable initial depolarisation in Stein's neuronal model with synaptic reversal potentials", Biological Cybernetics, 64, 285-291.
- Lansky P. and Rospars J.P. (1995) "Ornstein-Uhlenbeck model neuron revisited", Biol. Cybern. 72, 397-406.
- Mahowald M. and Douglas R. (1991) "A Silicon Neuron", Nature, 354, 515-518.
- Mason A., Nicol A. and Stratford K. (1991) "Synaptic transmission between individual pyramidal neurons of the rat visual-cortex invitro", Journal of Neuroscience, 11, 72-84.
- Parodi O., Combe Ph. and Ducom J.-C. (1995) "Temporal coding in vision: coding by the spike arrival time leads to oscillations in the case of moving targets", Biological Cybernetics, in press.
- Rospars J.P. and Lansky P. (1993) "Stochastic neuron model without resetting of dendritic potential: application to the olfactory system", Biological Cybernetics, 69, 283-294.
- Sejnowski T.J. (1986) "Open questions about computation in the cerebral cortex" in McClelland J.L. and Rumelhart D.E. (eds) "Parallel Distributed Processing, Vol. 2", 372-389, MIT Press.
- Shadlen M.N. and Newsome W.T. (1994) "Noise, neural codes and cortical organization", Current Opinion in Neurobiology, 4, 569-579.
- Shigematsu Y., Akiyama S. and Matsumoto G. (1992) "A spike-firing neural cell (SAM)", Extended Abstracts, 4th Int. Symp. on Bioelectronic and Molecular Electronic Devices, Miyazaki (edited by R & D Association for Future Electron Devices, Japan), 13-14.
- Smith D.R. and Smith D.K. (1965) "A statistical analysis of the continual activity of single cortical neurones in the cat unanaesthetized isolated forebrain", Biophys. J., 5, 47-74.

Softky W.R. and Koch C. (1993) "The highly irregular firing of cortical cells is inconsistent with temporal integration of random EPSPs", *J. Neuroscience*, 13, 334-350.

Softky W. (1994) "Sub-millisecond coincidence detection in active dendritic trees". *Neuroscience*, 58, 15-41.

Stein R.B. (1967) "Some models of neuronal variability", *Biophysics Journal*, 7, 37-68.

Stratford K., Mason A. Larkman A., Major G. and Jack J. (1989) "The modelling of pyramidal neurons in the visual cortex" in: Durbin R. et al. (eds) "The computing neuron", Addison-Wesley, Wokingham, 296-321.

Tsodyks M.V. and Sejnowski T. (1995) "Rapid state switching in balanced cortical network models", *Network*, 6, 111-124.

Usher M., Stemmler M., Koch C. and Olami Z. (1994) "Network amplification of local fluctuations causes high spike rate variability, fractal firing patterns and oscillatory local-field potentials", *Neural Computation*, 6, 795-836.

Zipser D., Kehoe B., Littlewort G and Fuster J. (1993) "A spiking network model of short-term active memory", *J. Neuroscience*, 13, 3406-3420.

Appendix A: Coefficient of variation of interspike intervals

A.1. Case with refractory time.

The coefficient of variation $CV(T)$ characterises the fluctuation of the time intervals between spikes compared to the average interval T :

$$CV(T) = \frac{\sigma(T)}{T} \quad [A1.1]$$

Where $\sigma(T)$ is the standard deviation of the interspike intervals, and T is the average interval. We will initially determine the value of $CV(T)$ in the case of discrete time steps Δt , then generalize to the continuous case in the limit $\Delta t \rightarrow 0$. In the discrete case, interspike intervals take values $T = k \cdot \Delta t$. The standard deviation $\sigma(T)$ of the interspike intervals is defined by

$$\sigma^2(T) = \sum_{T'=Tr+\Delta t}^{\infty} (T'-T)^2 P(T') = \Delta t^2 \sum_{k=kr+1}^{\infty} (k-\bar{k})^2 P(k) = \Delta t^2 \sigma^2(\bar{k}) \quad [A1.2]$$

Where $P(k)$ is the probability that interval k is observed. The minimum interval between two spikes is 1 (time step). The refractory time kr is defined here as the number of empty time steps following a spike. The minimum interval is $k_{min} = 1 + kr$ (see figure A1.1).



Figure A1.1: Illustration of the definitions of an interspike interval k and the refractory time kr ¹. (In this example $kr = 3$).

To design the expression for $P(k)$ we assume that, at each time step, there is a probability α of finding a spike, except during the refractory time when we are certain that no spike is produced. So, the probability of the event of an interval k , is given by the probability that no spike is produced from step $kr+1$ to step $k-1$ inclusive, i.e. during $k-1-kr$ time steps, and that a spike be produced at the k^{th} step. Thus the probability $P(k)$ is given by:

$$P(k) = (1 - \alpha)^{k-1-kr} \alpha \quad [A1.3]$$

To evaluate the variance of k (equation [A1.2]) we need to evaluate the average interspike interval \bar{k} :

$$\bar{k} = \sum_{k=1+kr}^{\infty} k P(k) = \frac{\alpha}{(1 - \alpha)^{kr}} \sum_{k=1+kr}^{\infty} (1 - \alpha)^{k-1} \quad [A1.4]$$

Using

$$k(1 - \alpha)^{k-1} = -\frac{\partial}{\partial \alpha} (1 - \alpha)^k \quad [A1.5]$$

¹ The figure reflects an older, more confusing notation where Tr was used instead of kr .

We find

$$\bar{k} = \frac{1 + \alpha kr}{\alpha} \quad [A1.6]$$

We may note that, when $kr = 0$, [A1.6] reduces to the expected results for a discrete Poisson process. To evaluate expression [A1.2] we also need \bar{k}^2 :

$$\bar{k}^2 = \sum_{k=1+kr}^{\infty} k^2 P(k) = \frac{\alpha}{(1-\alpha)^{kr}} \sum_{k=1+kr}^{\infty} k^2 (1-\alpha)^{k-1} \quad [A1.7]$$

Using

$$k^2 (1-\alpha)^{k-1} = (1-\alpha) \frac{\partial^2}{\partial \alpha^2} (1-\alpha)^k + k (1-\alpha)^{k-1} \quad [A1.8]$$

We find

$$\bar{k}^2 = \frac{1-\alpha}{\alpha^2} + \left(\frac{1}{\alpha} + kr\right)^2 \quad [A1.9]$$

Similarly we can also check that:

$$\sum_{k=kr+1}^{\infty} P(k) = 1 \quad [A1.10]$$

Finally, using [A1.10], [A1.9] and [A1.6], we can rewrite [A1.2]:

$$\sigma^2(k) = \bar{k}^2 - k^2 = \frac{1-\alpha}{\alpha} \quad [A1.11]$$

And the expression for the coefficient of variation [A1.1] becomes:

$$CV(k) = \sqrt{\frac{\sigma^2(k)}{\bar{k}^2}} = \frac{\sqrt{1-\alpha}}{1+\alpha kr} \quad [A1.12]$$

We may note that for $kr = 0$, [A1.12] reduces to the expression $CV = \sqrt{1-\alpha}$ given in [Christodoulou et al., 1994] for the coefficient of variation of spike trains produced by a pRAM neuron. To find the expression for the continuous case, we use

$$T = \bar{k} \Delta t = \left(kr + \frac{1}{\alpha}\right) \Delta t \quad [A1.13]$$

This also defines the relation between α and the actual mean interspike interval T :

$$\alpha = \frac{\Delta t}{T - kr \Delta t} = \frac{\Delta t}{T - Tr - \Delta t} \quad [A1.14]$$

This is obtained using the conventional definition of the refractory time as the minimum distance between two spikes $Tr = (kr + 1) \Delta t$.

Using [A1.1], [A1.2] and [A1.13] we note that $CV(T) = CV(k)$. Hence, from [A1.12], [A1.14] and the definition of Tr , and by setting Δt to zero, one finds:

$$CV(T) = \sqrt{\frac{T - Tr}{T}} \quad [A1.15]$$

A.2 Case with refractory time and bursting.

To estimate the effect of a bursting behaviour on the value of the coefficient of variation, we will make some simplifying assumptions. We assume that each burst contains γ spikes separated by the minimum interspike interval $1+Tr$ (See figure A2.1). We assume that bursts are produced according to an underlying process characterized by an interspike interval distribution $P(k)$. The only difference is that γ spikes are produced in place of one spike. To avoid the cases of overlapping spikes belonging to several bursts, we assume that the firing probability of the underlying process is very small: $\alpha \ll 1$.

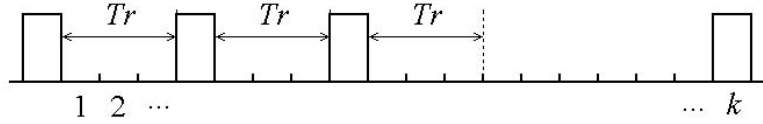


Figure A2.1: Illustration of the model for bursting. An underlying Poisson process with probability α generates the first spike of each burst. In the figure each burst contains $\gamma=3$ spikes. The duration of a burst is $\tau = (\gamma-1)(1+Tr)$. The interval which follows the burst would be k in the non-bursting case. Bursting reduces its duration to $k - \tau$.

To calculate the coefficient of variation, we need the average value T' of the interspike intervals. Let us denote by T the average interval in the non-bursting underlying process. In the bursting case there are γ intervals in the same duration. Therefore:

$$T' = \frac{T}{\gamma} \quad [A2.1]$$

We need also the new distribution $P'(k')$ of interspike intervals. A fraction $(\gamma-1)/\gamma$ of the intervals are of duration $1+Tr$. They belong to a distribution $P_1(k')$ having a single peak at $k'=1+Tr$. The remaining spikes, a fraction $1/\gamma$ of the total, belong to the original Poisson distribution $P(k)$, given in [A1.3], but shifted by a delay τ (Intervals which should have been of duration k appear shorter by a duration τ):

$$P'(k') = \frac{\gamma-1}{\gamma} P_1(k') + \frac{1}{\gamma} P(k'+\tau) \quad [A2.2]$$

with

$$P_1(k') = \begin{cases} 1 & \text{when } k' = 1+Tr \\ 0 & \text{otherwise} \end{cases} \quad [A2.3]$$

This allows us to calculate the average of the squared interspike intervals:

$$\overline{k'^2} = \sum_{k'=1+Tr}^{\infty} k'^2 P'(k') = \frac{\gamma-1}{\gamma} (1+Tr)^2 + \frac{1}{\gamma} \sum_{k'=1+Tr}^{\infty} k'^2 P(k'+\tau) \quad [A2.4]$$

Then, using $k''=k'+\tau$,

$$\overline{k'^2} = \frac{\gamma-1}{\gamma} (1+Tr)^2 + \frac{1}{\gamma} \sum_{k''=1+Tr+\tau}^{\infty} (k''-\tau)^2 P(k'') \quad [A2.5]$$

Then

$$\overline{k'^2} = \frac{\gamma-1}{\gamma}(1+Tr)^2 + \frac{1}{\gamma} \left[\sum_{k''=1+Tr+\tau}^{\infty} k''^2 P(k'') - 2\tau \sum_{k''=1+Tr+\tau}^{\infty} k'' P(k'') + \tau^2 \sum_{k''=1+Tr+\tau}^{\infty} P(k'') \right] \quad [A2.6]$$

We see that the effect of the bursts is to remove the lower part of the distribution $P(k)$ from the summation. Here we will use the assumption made earlier that there are no overlapping bursts. This is equivalent to say that the underlying Poisson process has a negligible probability to generate intervals smaller than τ . Therefore, the lower part of the distribution has a negligible contribution to the sums. Therefore, we can as well assume that the sum starts at $k''=1+Tr$.

This approximation allows to rewrite [A2.6]:

$$\overline{k'^2} = \frac{\gamma-1}{\gamma}(1+Tr)^2 + \frac{\overline{k''^2}}{\gamma} - \frac{2\tau\overline{k''}}{\gamma} + \frac{\tau^2}{\gamma} \quad [A2.7]$$

If we know the coefficient of variation $CV(T)_{Underlying}$ of the underlying distribution $P(k)$, which is defined by:

$$CV(T)_{Underlying}^2 = \frac{\overline{k''^2} - \overline{k''}^2}{\overline{k''}^2} \quad [A2.8]$$

then we can write

$$\overline{k''^2} = \overline{k''}^2 (CV(T)_{Underlying}^2 + 1) \quad [A2.9]$$

and rewrite [A2.7] as:

$$\overline{k'^2} = \frac{\gamma-1}{\gamma}(1+Tr)^2 + \frac{T^2}{\gamma} (CV(T)_{Underlying}^2 + 1) - \frac{2T\tau}{\gamma} + \frac{\tau^2}{\gamma} \quad [A2.10]$$

The new coefficient of variation, due to bursting, becomes:

$$CV(T')_{Burst}^2 = \frac{\overline{k'^2} - \overline{k'}^2}{\overline{k'}^2} = \frac{\gamma^2}{T^2} \left(\frac{\gamma-1}{\gamma}(1+Tr)^2 + \frac{T^2}{\gamma} (CV(T)_{Underlying}^2 + 1) - \frac{2T\tau}{\gamma} + \frac{\tau^2}{\gamma} - \frac{T^2}{\gamma^2} \right) \quad [A2.11]$$

By neglecting terms of the order of $(1/T^2)$, by remembering that the measured interspike interval is given by $T'=T/\gamma$ and that $\tau=(\gamma-1)(1+Tr)$, we find:

$$CV(T')_{Burst}^2 \cong \gamma(CV(T)_{Underlying}^2 + 1) - \frac{2(\gamma-1)(1+Tr)}{T'} - 1 \quad [A2.12]$$

If the underlying process is a Poisson process, [A2.12] reduces to:

$$CV(T')_{Burst}^2 \cong 2\gamma - \frac{2(\gamma-1)(1+Tr)}{T'} - 1 \quad [A2.13]$$

We see that for $\gamma=1$, i.e. when there are no bursts [A2.13] reduces to $CV=1$, an expected result.

Appendix B: Counting statistics

B.1 Case without refractory time or bursting.

Determining the variance $VAR(N)$ of the number of spikes counted during a time window W is a way to characterize the variability of the firing of a neuron [Dean, 1981]. Here N represents the average of the number of counted spikes. The variance is defined by:

$$VAR(N) = \overline{n^2} - \bar{n}^2 \quad [B1.1]$$

Where \bar{n} is the average of the number of spikes counted during a series of successive time-windows of length W . It is equivalent to N . As we operate in discrete time steps, we will characterize W by a number of time steps w . In general \bar{n} is given by:

$$\bar{n} = \sum_{n=0}^w n P(n) \quad [B1.2]$$

Where $P(n)$ is the probability that a number n of spikes is counted in w time-steps. As there is at most one spike per time-step, the maximum counted number of spikes is w . If we assume that there is a probability α to observe a spike at each step (or to produce a spike), then:

$$P(n) = \binom{w}{n} \alpha^n (1-\alpha)^{w-n} \quad [B1.3]$$

which is the probability of having exactly n steps with a spike and $w-n$ steps without. The term $\binom{w}{n} = \frac{w!}{n!(w-n)!}$ counts the number of combinations of n spikes in w steps which all contribute to $P(n)$. Using [B1.3] one can rewrite [B1.2]:

$$\bar{n} = (1-\alpha)^w \sum_{n=0}^w \binom{w}{n} n \left(\frac{\alpha}{1-\alpha}\right)^n \quad [B1.4]$$

using $x = \alpha/(1-\alpha)$, reminding that $nx^n = x \frac{\partial}{\partial x} x^n$ and that $\sum_{n=0}^w \binom{w}{n} a^n b^{w-n} = (a+b)^w$ we find:

$$\bar{n} = (1-\alpha)^w x \frac{\partial}{\partial x} \sum_{n=0}^w \binom{w}{n} x^n = (1-\alpha)^w x \frac{\partial}{\partial x} (x+1)^w = \alpha w \quad [B1.5]$$

Using the same techniques and expression $n^2 x^n = x^2 \frac{\partial^2}{\partial x^2} x^n + nx^n$ one finds:

$$\overline{n^2} = \sum_{n=0}^w n^2 P(n) = (1-\alpha)^w \sum_{n=0}^w \binom{w}{n} n^2 \left(\frac{\alpha}{1-\alpha}\right)^n = \alpha w (1 + \alpha w - \alpha) \quad [B1.6]$$

Finally, the variance can be calculated from [B1.1], [B1.5] and [B1.6]:

$$VAR(N) = \alpha w (1-\alpha) = N \left(1 - \frac{N}{w}\right) \quad [B1.7]$$

This equation shows that, for a discrete Poisson process, as assumed here, the variance of N is essentially equal to N . The term $(1-\alpha)$ is due to the discrete nature of the time scale and disappears in the continuous limit, when $\alpha \ll 1$.

B.2 Case with refractory time in the low frequency limit.

The main problem which needs to be solved here is the determination of the new expression for $P(n)$. Let us look first at the number of combinations C_n^w of n spikes in a time window of w time steps. The first spike can be placed in $L_1 = w - Tr$ steps. Tr steps are deduced to avoid that refractory periods of spikes in one time window overflow into the next time window. As for the second spike, we assume that there are w_1 free steps to the left of the first spike, and w_2 free steps to the right of the refractory time of the first spike (as in figure B2.1).

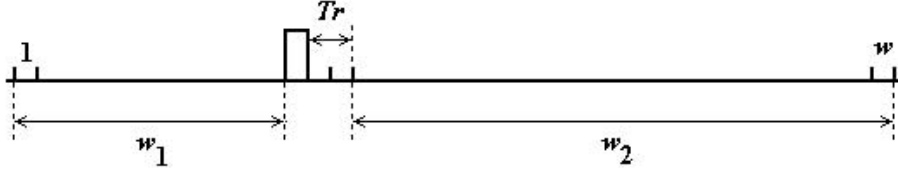


Figure B2.1: Illustration of the definition of free time steps w_1 and w_2 available for the second spike.

Using the same argument of non-overflowing refractory periods, in these w_1 and w_2 steps there are $L_2 = (w_1 - Tr) + (w_2 - Tr)$ possible positions for the second spike. Indeed, this expression makes no sense when one or both of the time windows are smaller than Tr . To eliminate this case, we will consider only the *low frequency limit* characterised by $w \gg n$. A more precise definition of this limit will be given after equation [B2.X]. As $w_1 + w_2 = w - Tr - 1$, we can rewrite $L_2 = w - 3Tr - 1$. In general:

$$L_m = w - (m-1)(Tr+1) - mTr = w + Tr + 1 - m(2Tr+1) \quad [B2.1]$$

We may note that according to expression [B2.1], the maximum possible number of spikes that can be placed is $m_{\max} = (w - Tr) / (2Tr + 1)$, which is approximately half of the true maximum number of spikes and their refractory time which one could place in an orderly way in w steps, i.e. $w / (Tr + 1)$. (m_{\max} is reached when there is only one possible position left for that spike: $L_{m_{\max}} = 1$).

Remembering that the number of indistinguishable configurations (permutations) of n spikes is $n!$, the total number of distinguishable possible configurations of n spikes is given by:

$$C_n^w = \frac{1}{n!} \prod_{m=1}^n L_m = \frac{1}{n!} \prod_{m=1}^n \{w - (m-1)(Tr+1) - mTr\} = \frac{1}{n!} \prod_{m=1}^n \{w + Tr + 1 - m(2Tr+1)\} \quad [B2.1]$$

To rewrite this expression using factorials one has to pull the term $2Tr + 1$ out of the product. This is only possible if $w + Tr + 1$ is an integer multiple of $2Tr + 1$. Such an assumption does not affect notably the validity of the results. So let us make such a restriction. Thus

$$C_n^w = \frac{(2Tr+1)^n}{n!} \prod_{m=1}^n \left\{ \frac{w+Tr+1}{2Tr+1} - m \right\} = \frac{(2Tr+1)^n}{n!} \frac{\delta!}{(\delta-n)!} \quad [B2.2]$$

where $\delta = (w - Tr) / (2Tr + 1) = m_{\max}$.

Let us now turn to the probability $P(n)$ of observing exactly n spikes in w time steps. After n spikes have been placed, a number L_{n+1} of free positions remains for spikes. Thus, the

probability of observing exactly n spikes is the probability of having n spikes in n time steps and no spikes in L_{n+1} steps:

$$P(n) = C_n^w \alpha^n (1-\alpha)^{L_{n+1}} = \frac{(2Tr+1)^n}{n!} \frac{\delta!}{(\delta-n)!} \alpha^n (1-\alpha)^{(\delta-n)(2Tr+1)} \quad [B2.3]$$

In order to produce a tractable expression of $P(n)$, we introduce another approximation. It is known that:

$$(1+x)^{\frac{q}{m}} = 1 + \frac{q}{m}x - \frac{q(m-q)}{2!m^2}x^2 + \frac{q(m-q)(2m-q)}{3!m^3}x^3 + \dots + (-1)^k \frac{q(m-q)(2m-q)\dots((k-1)m-q)}{k!m^k}x^k + \dots \quad [B2.4]$$

If $m \ll q$ and if $x < 1$ (so that the terms with large values of k do not contribute and $km \ll q$) then:

$$(1+x)^{\frac{q}{m}} \cong 1 + \frac{q}{m}x - \frac{q(-q)}{2!} \left(\frac{x}{m}\right)^2 + \frac{q(-q)(-q)}{3!} \left(\frac{x}{m}\right)^3 + \dots + (-1)^k \frac{q(-q)(-q)\dots(-q)}{k!} \left(\frac{x}{m}\right)^k + \dots \quad [B2.5]$$

If $q \gg 1$, then we can add small constants in the brackets:

$$\begin{aligned} (1+x)^{\frac{q}{m}} &\cong 1 + q \frac{x}{m} - \frac{q(1-q)}{2!} \left(\frac{x}{m}\right)^2 + \frac{q(1-q)(2-q)}{3!} \left(\frac{x}{m}\right)^3 + \dots + (-1)^k \frac{q(1-q)(2-q)\dots((k-1)-q)}{k!} \left(\frac{x}{m}\right)^k + \dots \\ &\cong \left(1 + \frac{x}{m}\right)^q \end{aligned} \quad [B2.6]$$

So, provided that i) $\alpha < 1$, ii) $(\delta-n) \gg 1/(2Tr+1)$ and iii) $(\delta-n) \gg 1$, we can use [B2.6] to write

$$(1-\alpha)^{(\delta-n)(2Tr+1)} \cong (1-(2Tr+1)\alpha)^{\delta-n} \quad [B2.7]$$

The condition (i) is equivalent to the low frequency limit assumption made earlier. The condition (ii) is always verified if condition (iii) is verified. Condition (iii) requires that $\delta \gg n$, which means that the actual number of spikes n must be much smaller than m_{\max} . For instance with $w=500\text{ms}$ and $Tr=1\text{ms}$, we find $m_{\max} = 166$. So, as long as we consider spike trains with much less than 166 spikes per 500ms, we can use [B2.7] to rewrite [B2.3]:

$$P(n) \cong \binom{\delta}{n} b^n (1-b)^{\delta-n} \quad [B2.8]$$

where $b=(2Tr+1)\alpha$. Using this expression, we can start to evaluate the terms needed to calculate the variance of the number of spikes counted in w time steps. From [B1.2] and by analogy with [B1.5], the average number of spikes can be written:

$$\bar{n} = \sum_{n=0}^w \binom{\delta}{n} n b^n (1-b)^{\delta-n} \cong \sum_{n=0}^{\delta} \binom{\delta}{n} n b^n (1-b)^{\delta-n} = b\delta = \alpha(w-Tr) \quad [B2.9]$$

We may note the reduction of the range of the summation from $\{0, w\}$ to $\{0, \delta\}$. This is consistent with the assumption that the number of spikes in w is much smaller than δ . Similarly, we calculate the average of the square of the number of spikes found in w . By analogy with [B1.6], we find :

$$\begin{aligned} \overline{n^2} &= \sum_{n=0}^w \binom{\delta}{n} n^2 b^n (1-b)^{\delta-n} \cong \sum_{n=0}^{\delta} \binom{\delta}{n} n^2 b^n (1-b)^{\delta-n} = b\delta(1+b(\delta-1)) \\ &= \alpha(w-Tr) + \alpha^2(w-Tr)^2 - \alpha^2(w-Tr)(1+2Tr) \end{aligned} \quad [B2.10]$$

Using [B2.9] and [B2.10], and reminding that N is the average value of n , the variance can be calculated:

$$\text{VAR} (N) = \overline{n^2} - \bar{n}^2 \cong \alpha(w - Tr)[1 - \alpha - 2\alpha Tr] = N(1 - \alpha(1 + 2Tr)) \quad [B2.11]$$

When compared to [B2.7], this expression shows an earlier decrease of the variance at high frequencies, due to the higher regularity of the interspike intervals imposed by the refractory time. We may note that this effect persists for $Tr=0$, suggesting that discrete time steps have effects similar to those of a refractory time. Reminding from [B2.9] that $\alpha = N/(w - Tr)$ we eventually find

$$\text{VAR} (N) \cong N\left(1 - \frac{N}{w - Tr}(1 + 2Tr)\right) \cong N - N^2 \frac{1 + 2Tr}{w} \quad [B2.12]$$

B.3 Case with refractory time and bursting.

The effect of bursting is much simpler to introduce in an expression of the variance of the spike count N' than in the expression of the coefficient of variation of the interspike interval, as done in Appendix A2. Here we assume, as in Appendix A2, that bursts are composed of γ spikes separated by Tr time steps. Bursts are generated by a Poisson process characterised by a probability α of generating a burst at each time step. To avoid overlapping bursts, we operate also in the low frequency limit where $N' \ll w$ and N' is the average number of spikes counted in w time-steps.

With these assumptions we know that every time we observe n' spikes produced by a bursting neuron in a time w , there would have been n'/γ spikes produced by the non-bursting neuron described in Appendix B2. So, the probability $P'(n')$ of observing n' spikes in the bursting case is the same as the probability $P(n'/\gamma)$ of observing n'/γ spikes in the non-bursting case [B2.8]:

$$P'(n') = P(n'/\gamma) \quad [B3.1]$$

We know also that the number n' of spikes observed in the bursting case is a multiple of the number of spikes in a burst:

$$n' = n\gamma \quad [B3.2]$$

Therefore, the variance $VAR_{Burst}(N')$ in the bursting case can be rewritten as a function of the variance $VAR_{Poisson}(N)$ in the non-bursting case:

$$VAR_{Burst}(N') = \sum_{n'=0}^w (\bar{n}' - n')^2 P'(n') = \sum_{n=0}^{w/\gamma} \gamma^2 (\bar{n} - n)^2 P(n) \cong \gamma^2 VAR_{Poisson}(N) \quad [B3.3]$$

We may note the reduction of the summation range from $\{0, w\}$ to $\{0, w/\gamma\}$. This bears no consequences if the low frequency assumption $\gamma N \ll w$ is respected. So far, we have not used the explicit form of the underlying distribution $P(n)$. Therefore, result [B3.3] is valid for any distribution $P(n)$. Using the expression for $VAR_{Poisson}(N)$ given in [B2.11] and remembering that $N' = \gamma N$, we can rewrite [B3.3]:

$$VAR_{Burst}(N') \cong \gamma N'(1 - \alpha(1 + 2Tr)) \cong \gamma N' \quad [B3.4]$$

Note that α characterises the underlying Poisson process. Therefore $\alpha = N'/\gamma w$. However, as expression [B3.4] is only valid in the low frequency limit, the term containing α can be neglected in most practical applications. We may also note that details of the intervals between spikes in bursts are not critical. It has been shown that expression [B3.3] is also valid in the case of clusters of spikes overlapping with each others, in the limit of large values of w [Gruneis et al, 1989].